arXiv:1407.8522v3 [hep-ph] 23 Oct 2014

RECONCILING INDUCED-GRAVITY INFLATION IN SUPERGRAVITY WITH THE *Planck* 2013 & BICEP2 RESULTS

C. PALLIS

Departament de Física Teòrica and IFIC,
Universitat de València-CSIC,
E-46100 Burjassot, SPAIN

ABSTRACT

We generalize the embedding of induced-gravity inflation beyond the no-scale Supergravity presented in Ref. [1] employing two gauge singlet chiral superfields, a superpotential uniquely determined by applying a continuous R and a discrete $\mathbb{Z}_n$ symmetries, and a logarithmic Kähler potential including all the allowed terms up to fourth order in powers of the various fields. We show that, increasing slightly the prefactor (-3) encountered in the adopted Kähler potential, an efficient enhancement of the resulting tensor-to-scalar ratio can be achieved rendering the predictions of the model consistent with the recent BICEP2 results, even with subplanckian excursions of the original inflaton field. The remaining inflationary observables can become compatible with the data by mildly tuning the coefficient involved in the fourth order term of the Kähler potential which mixes the inflaton with the accompanying non-inflaton field. The inflaton mass is predicted to be close to 10^{14} GeV.

Keywords: Cosmology, Supersymmetric models, Supergravity, Modified Gravity;
PACS codes: 98.80.Cq, 11.30.Qc, 12.60.Jv, 04.65.+e, 04.50.Kd

Dedicated to the memory of my High School teacher, V. Aspiotis.

Published in *J. Cosmol. Astropart. Phys.* **10**, 058 (2014)

CONTENTS

1 INTRODUCTION **1**
2 GENERALIZING THE EMBEDDING OF THE IG INFLATION IN SUGRA **2**
3 THE INFLATIONARY SCENARIO **3**
3.1 THE INFLATIONARY POTENTIAL 4
3.2 THE INFLATIONARY REQUIREMENTS 6
3.3 ANALYTIC RESULTS 7
3.4 NUMERICAL RESULTS 9
4 THE EFFECTIVE CUT-OFF SCALE **12**
5 CONCLUSIONS **13**
REFERENCES **14**

1 INTRODUCTION

Although compatible with the *Planck* (and WMAP) data [2], the models of *induced-gravity* (IG) inflation [3] formulated within standard *Supergravity* (SUGRA) yield [1] a low tensor-to-scalar ratio $r \simeq 0.004$ which fails to approach the recent BICEP2 results [4] – for other recent incarnations of IG inflation see Ref. [5, 6]. More specifically, the BICEP2 collaboration has detected a B-mode in the polarization of the cosmic microwave background radiation at large angular scales. If this observation is attributed to the primordial gravity waves predicted by inflation, it implies [4] $r = 0.16^{+0.06}_{-0.05}$ – after substraction of a dust foreground. Despite the fact that this result is subject to considerable uncertainties [7,8] and its interpretation as a detection of primordial gravitational waves becomes more and more questionable [9], it motivates us to explore how IG inflation can also accommodate large r's – for similar recent attempts see Ref. [10–12]. In particular, taking into account both the *Planck* [2] and BICEP2 [4] data we find a simultaneously compatible region [13]

$$0.06 \lesssim r \lesssim 0.135 \tag{1.1}$$

at 95% *confidence level* (c.l.) which can be considered as the most exciting region where r values may be confined for models with low running, $a_{\rm s}$, of the (scalar) spectral index, $n_{\rm s}$.

In this paper we show that modifying modestly the implementation of IG inflation beyond the no-scale SUGRA [14] we can ensure a sizable augmentation of the resulting r's *with respect to* (w.r.t) those obtained in the models presented in Ref. [1]. The key-ingredient of our generalization is the variation of the numerical prefactor encountered in the adopted Kähler potential. We show that increasing the conventional value (-3) of this prefactor by an amount of order 0.01, the inflationary potential acquires a moderate inclination accommodating, thereby, observable r's reconcilable with Eq. (1.1). In this set-up IG inflation, although less predictive than its realization in no-scale SUGRA, preserves a number of attractive features [1, 15]. Most notably, the super- and Kähler potentials are fixed by an R and a discrete $\mathbb{Z}_n$ symmetries, inflation is realized using subplanckian values of the initial (non-canonically normalized) inflaton field, the radiative corrections remain under control and the perturbative unitarity is respected up to the reduced Planck scale, $m_{\rm P} = 2.44 \cdot 10^{18}$ GeV [1, 15, 16].

Below we generalize in Sec. 2 the formulation of IG inflationary models within SUGRA. In Sec. 3 we present the basic ingredients of these models, derive the inflationary observables and test them against observations. We end-up with a brief analysis of the UV behavior of these models in Sec. 4 and the summary of our conclusions in Sec. 5. Throughout we follow closely the notation and the conventions adopted in Ref. [1], whose Sections, Equations, Tables and Figures are referred including a prefix "R.1". E.g. Eq. (R.1-3.6) denotes Eq. (3.6) of Ref. [1].

2 GENERALIZING THE EMBEDDING OF THE IG INFLATION IN SUGRA

According to the scheme proposed in Ref. [1], the implementation of IG inflation in SUGRA requires at least two singlet superfields, i.e., $z^\alpha = \Phi, S$, with Φ ($\alpha = 1$) and S ($\alpha = 2$) being the inflaton and a stabilized field respectively. The superpotential W of the model has the form

$$W = \frac{\lambda m_{\rm P}^2}{c_{\mathcal{R}}} S\left(\Omega_{\rm H} - 1/2\right) \quad \text{with} \quad \Omega_{\rm H}(\Phi) = c_{\mathcal{R}}\frac{\Phi^n}{m_{\rm P}^n} + \sum_{k=1}^{\infty}\lambda_k\frac{\Phi^{2kn}}{m_{\rm P}^{2kn}} \tag{2.1}$$

which is (i) invariant under the action of a global $\mathbb{Z}_n$ discrete symmetry, i.e.,

$$W \to \ W \ \text{ for } \ \Phi \ \to \ -\Phi\,, \tag{2.2}$$

and (ii) consistent with a continuous R symmetry under which

$$W \to \ e^{i\varphi}\, W \ \text{ for } \ S \ \to \ e^{i\varphi}\, S \ \text{ and } \ \Omega_{\rm H} \ \to \ \Omega_{\rm H}\,. \tag{2.3}$$

Confining ourselves to $\Phi < m_{\rm P}$ and assuming relatively low λ_k's we hereafter neglect the second term in the definition of $\Omega_{\rm H}$ in Eq. (2.1). As shown in Ref. [1], W in Eq. (2.1) leads to a spontaneous breaking of $\mathbb{Z}_n$ at the SUSY vacuum which lies at the direction

$$\langle S\rangle = 0 \ \text{ and } \ \langle\Omega_{\rm H}\rangle = 1/2, \tag{2.4}$$

where we take into account that the phase of Φ, $\arg\Phi$, is stabilized to zero. If $\Omega_{\rm H}$ is the holomorphic part of the frame function Ω and dominates it, Eq. (2.4) assures a transition to the conventional Einstein gravity realizing, thereby, the idea of IG [3]. Our main point in this paper is that this construction remains possible for a broad class of relations between Ω and the Kähler potential K.

Indeed, if we perform a conformal transformation defining the JF metric $g_{\mu\nu}$ through the relation

$$\widehat{g}_{\mu\nu} = -\frac{\Omega}{3(1+m)}g_{\mu\nu} \ \Rightarrow \ \begin{cases}\sqrt{-\widehat{\mathfrak{g}}} = \frac{\Omega^2}{9(1+m)^2}\sqrt{-\mathfrak{g}} \ \text{ and } \ \widehat{g}^{\mu\nu} = -\frac{3(1+m)}{\Omega}g^{\mu\nu},\\ \widehat{\mathcal{R}} = -\frac{3(1+m)}{\Omega}\left(\mathcal{R} - \Box\ln\Omega + 3g^{\mu\nu}\partial_\mu\Omega\partial_\nu\Omega/2\Omega^2\right)\end{cases} \tag{2.5}$$

where m is a dimensionless (small in our approach) parameter which quantifies the deviation from the standard set-up [17], the EF action

$$\mathsf{S} = \int d^4x\sqrt{-\widehat{\mathfrak{g}}}\left(-\frac{1}{2}m_{\rm P}^2\widehat{\mathcal{R}} + K_{\alpha\bar\beta}\widehat{g}^{\mu\nu}\partial_\mu z^\alpha\partial_\nu z^{*\bar\beta} - \widehat{V}\right), \tag{2.6}$$

– where $\widehat{V}$ is the F–term SUGRA scalar potential given below –, is written in the JF as follows [17]

$$\mathsf{S} = \int d^4x\sqrt{-\mathfrak{g}}\left(\frac{m_{\rm P}^2\Omega\mathcal{R}}{6(1+m)} + \frac{m_{\rm P}^2}{4(1+m)\Omega}\partial_\mu\Omega\partial^\mu\Omega - \frac{1}{(1+m)}\Omega K_{\alpha\bar\beta}\partial_\mu z^\alpha\partial^\mu z^{*\bar\beta} - V\right) \tag{2.7}$$

with $V = \frac{\Omega^2}{9(1+m)^2}\widehat{V}$ being the JF potential. If we specify the following relation between Ω and K,

$$-\Omega/3(1+m) = e^{-K/3(1+m)m_{\rm P}^2} \ \Rightarrow \ K = -3(1+m)m_{\rm P}^2\ln\left(-\Omega/3(1+m)\right), \tag{2.8}$$

and employ the definition [17] of the purely bosonic part of the on-shell value of the auxiliary field

$$\mathcal{A}_\mu = i\left(K_\alpha\partial_\mu z^\alpha - K_{\bar\alpha}\partial_\mu z^{*\bar\alpha}\right)/6, \tag{2.9}$$

we arrive at the following action

$$\mathsf{S}=\int d^4x\sqrt{-\mathfrak{g}}\left(\frac{m_{\rm P}^2\Omega\mathcal{R}}{6(1+m)}+m_{\rm P}^2\left(\Omega_{\alpha\bar{\beta}}-\frac{m\Omega_\alpha\Omega_{\bar{\beta}}}{(1+m)\Omega}\right)\partial_\mu z^\alpha\partial^\mu z^{*\bar{\beta}}-\frac{\Omega\mathcal{A}_\mu\mathcal{A}^\mu}{(1+m)^3m_{\rm P}^2}-V\right), \tag{2.10}$$

where $\mathcal{A}_\mu$ in Eq. (2.9) takes the form

$$\mathcal{A}_\mu=-i(1+m)m_{\rm P}^2\left(\Omega_\alpha\partial_\mu z^\alpha-\Omega_{\bar{\alpha}}\partial_\mu z^{*\bar{\alpha}}\right)/2\Omega\,. \tag{2.11}$$

It is clear that Eqs. (2.10) and (2.11) reduce to Eqs. (R.1-2.3) and (R.1-2.4) respectively for $m=0$. The choice $m\neq 0$, although not standard, is perfectly consistent with the idea of IG. Indeed, as in Ref. [1] we adopt the following form for the frame function

$$-\Omega/3(1+m)=\Omega_{\rm H}(\Phi)+\Omega_{\rm H}{}^*(\Phi^*)-\Omega_{\rm K}\left(|\Phi|,|S|\right)/3(1+m), \tag{2.12a}$$

where $\Omega_{\rm K}$ includes the kinetic terms for the z^α's and takes the form

$$\Omega_{\rm K}\left(|\Phi|,|S|\right)=\frac{|S|^2+|\Phi|^2}{m_{\rm P}^2}-\frac{k_S|S|^4+2k_\Phi|\Phi|^4+2k_{S\Phi}|S|^2|\Phi|^2}{m_{\rm P}^4}, \tag{2.12b}$$

with sufficiently small coefficients $k_{\alpha\beta}$ i.e. $k_{\alpha\beta}\ll c_{\mathcal{R}}$. As a consequence, $\Omega_{\rm H}$ represents the non-minimal coupling to gravity and so Eq. (2.4) dynamically generates $m_{\rm P}$. As for $m=0$, when the dynamics of the z^α's is dominated only by the real moduli $|z^\alpha|$ or if $z^\alpha=0$ for $\alpha\neq 1$ [17], we can obtain $\mathcal{A}_\mu=0$ in Eq. (2.10). The only difference w.r.t the case with $m=0$ is that now the scalar fields z^α have not canonical kinetic terms in the JF due to the term proportional to $\Omega_\alpha\Omega_{\bar{\beta}}\neq\delta_{\alpha\bar{\beta}}$. This fact does not cause any problem, since the canonical normalization of the inflaton keeps its strong dependence on $c_{\mathcal{R}}$ included in $\Omega_{\rm H}$ whereas the non-inflaton fields become heavy enough during inflation and so, they do not affect the dynamics – see Sec. 3.1. Note that our present set-up lies on beyond the no-scale SUGRA embedding of IG inflation since the framework of the no-scale SUGRA [14] is defined by supplementing Eq. (R.1-2.8) with the imposition $m=0$. Indeed, only under this condition the cosmological constant term into the EF F–term SUGRA scalar potential – see below – vanishes.

The resulting through Eq. (2.8) Kähler potential is

$$K=-3(1+m)m_{\rm P}^2\ln\left(\Omega_{\rm H}+\Omega_{\rm H}^*-\frac{|S|^2+|\Phi|^2}{3(1+m)m_{\rm P}^2}+\frac{k_S|S|^4+2k_\Phi|\Phi|^4+2k_{S\Phi}|S|^2|\Phi|^2}{3(1+m)m_{\rm P}^4}\right). \tag{2.13}$$

Recall that the fourth order term for S is included to cure the problem of a tachyonic instability occurring along this direction [17] and the remaining terms of the same order are considered for consistency – the factors of 2 are added just for convenience. Alternative solutions to the aforementioned problem of the tachyonic instability are recently identified in Ref. [18–20].

3 THE INFLATIONARY SCENARIO

In this section we describe the inflationary potential of our model in Sec. 3.1. We then exhibit a number of constraints imposed (Sec. 3.2) and present our analytic and numerical results in Sec. 3.3 and 3.4 respectively.

3.1 THE INFLATIONARY POTENTIAL

The EF F–term (tree level) SUGRA scalar potential, $\widehat{V}_{\rm IG0}$, of IG inflation is obtained from W and K in Eqs. (2.1) and (2.13) respectively by applying (for $z^\alpha = \Phi, S$) the well-known formula

$$\widehat{V}_{\rm IG0} = e^{K/m_{\rm P}^2}\left(K^{\alpha\bar{\beta}}{\rm F}_\alpha {\rm F}^*_{\bar{\beta}} - 3\frac{|W|^2}{m_{\rm P}^2}\right) = e^{K/m_{\rm P}^2}K^{SS^*}\,|W_{,S}|^2 = \frac{\lambda^2 m_{\rm P}^4 |2\Omega_{\rm H}-1|^2}{4c_{\mathcal R}^2 f_{S\Phi} f_{\mathcal R}^{2+3m}}\,, \tag{3.1a}$$

where ${\rm F}_\alpha = W_{,z^\alpha} + K_{,z^\alpha}W/m_{\rm P}^2$ and S is placed at the origin. Here we take into account that

$$e^{K/m_{\rm P}^2} = f_{\mathcal R}^{-3(1+m)} \;\;\text{and}\;\; K^{SS^*} = f_{\mathcal R}/f_{S\Phi}. \tag{3.1b}$$

The functions $f_{\mathcal R}$ and $f_{S\Phi}$, defined as follows – cf. Eq. (R.1-3.26):

$$f_{\mathcal R} = -\frac{\Omega}{3(1+m)} = 2c_{\mathcal R}\frac{x_\phi^n}{2^{n/2}} + \frac{x_\phi^2}{6(1+m)} + \frac{k_\Phi}{12(1+m)}x_\phi^4; \tag{3.1c}$$

$$f_{S\Phi} = m_{\rm P}^2\Omega_{,SS^*} = 1 - k_{S\Phi}x_\phi \;\;\text{with}\;\; x_\phi = \phi/m_{\rm P}, \tag{3.1d}$$

are computed along the inflationary track, i.e., for

$$\theta = s = \bar{s} = 0, \tag{3.2}$$

using the standard parametrization for Φ and S

$$\Phi = \frac{\phi}{\sqrt{2}}\,e^{i\theta/m_{\rm P}} \;\;\text{and}\;\; S = \frac{s+i\bar{s}}{\sqrt{2}}\,\cdot \tag{3.3}$$

Given that $f_{S\Phi} \ll f_{\mathcal R} \simeq 2\Omega_{\rm H}$ with $c_{\mathcal R} \gg 1$, $\widehat{V}_{\rm IG0}$ in Eq. (3.1a) is roughly proportional to x_ϕ^{-3mn}. Besides the inflationary plateau which emerges for $m = 0$ and studied in Ref. [1], a chaotic-type potential (bounded from below) is generated for $m < 0$. More specifically, $\widehat{V}_{\rm IG0}$ can be cast in the following from – cf. Eq. (R.1-3.25a):

$$\widehat{V}_{\rm IG0} = \frac{\lambda^2 m_{\rm P}^4 f_n^2 x_\phi^{-6m}\left(2^{1-n/2}c_{\mathcal R}x_\phi^{n-2} - f_{\phi\phi}/6(1+m)\right)^{-3m}}{4c_{\mathcal R}^2 x_\phi^4\left(c_{\mathcal R}x_\phi^{n-2} - 2^{n/2-1}f_{\phi\phi}/6(1+m)\right)^2 f_{S\Phi}}, \tag{3.4}$$

where $f_{\phi\phi} = 1 - k_\Phi x_\phi^2$ and $f_n = (2^{n/2-1} - c_{\mathcal R}x_\phi^n)$ coincides with $f_{\phi\phi}$ and f_Φ defined in Eq. (R.1-3.10). Confining ourselves to $n = 2$ – which, as we justify in Sec. 3.4 consists the most interesting choice – $\widehat{V}_{\rm IG0}$ takes the form

$$\widehat{V}_{\rm IG0} = \frac{\lambda^2 m_{\rm P}^4 f_2^2 x_\phi^{-6m}}{4c_{\mathcal R}^2 x_\phi^4 f_{S\Phi}}\left(c_{\mathcal R} - \frac{f_{\phi\phi}}{6(1+m)}\right)^{-(2+3m)} \simeq \frac{\lambda^2 m_{\rm P}^4 x_\phi^{-6m}}{4f_{S\Phi}c_{\mathcal R}^{2+3m}}\,, \tag{3.5}$$

whereas the corresponding EF Hubble parameter is

$$\widehat{H}_{\rm IG} = \frac{\widehat{V}_{\rm IG0}^{1/2}}{\sqrt{3}m_{\rm P}} \simeq \frac{\lambda m_{\rm P} x_\phi^{-3m}}{2\sqrt{3f_{S\Phi}}c_{\mathcal R}^{1+3m/2}}\,\cdot \tag{3.6}$$

The stability of the configuration in Eq. (3.2) can be checked verifying the validity of the conditions

$$\partial\widehat{V}_{\rm IG0}/\partial\widehat{\chi}^\alpha = 0 \;\;\text{and}\;\; \widehat{m}^2_{\chi^\alpha} > 0 \;\;\text{with}\;\; \chi^\alpha = \theta, s, \bar{s}, \tag{3.7}$$

FIELDS	EINGESTATES	MASSES SQUARED
1 real scalar	$\widehat{\theta}$	$\widehat{m}_\theta^2 \simeq \lambda^2 m_{\rm P}^2 \left(2 - 2c_{\mathcal{R}} x_\phi^2 f_2 + 3m f_2^2\right)$ $/6(1+m)c_{\mathcal{R}}^{4+3m} x_\phi^{2(2+3m)} \simeq 4\widehat{H}_{\rm IG}^2$
2 real scalars	$\widehat{s},\ \widehat{\bar{s}}$	$\widehat{m}_s^2 = \lambda^2 m_{\rm P}^2 \left(2 - 6m - c_{\mathcal{R}} x_\phi^2 + 6k_S(1+m) f_2^2\right)$ $/6(1+m)c_{\mathcal{R}}^{3(1+m)} x_\phi^{2(1+3m)}$
2 Weyl spinors	$\widehat{\psi}_\pm = \frac{\widehat{\psi}_\Phi \pm \widehat{\psi}_S}{\sqrt{2}}$	$\widehat{m}_{\psi\pm}^2 \simeq \lambda^2 m_{\rm P}^2 (2+3mf_2)^2/12(1+m)c_{\mathcal{R}}^{4+3m} x_\phi^{2(2+3m)}$

Table 1: *The mass spectrum along the inflationary trajectory in Eq. (3.2) for $m < 0$ and $n = 2$ in Eqs. (2.1) and (2.13).*

where $\widehat{m}_{\chi^\alpha}^2$ are the eigenvalues of the mass matrix with elements $\widehat{M}_{\alpha\beta}^2 = \partial^2 \widehat{V}_{\rm IG0}/\partial\widehat{\chi}^\alpha \partial\widehat{\chi}^\beta$ and hat denotes the EF canonically normalized fields defined by the kinetic terms in Eq. (2.6) as follows

$$K_{\alpha\bar{\beta}} \dot{z}^\alpha \dot{z}^{*\bar{\beta}} = \frac{1}{2}\left(\dot{\widehat{\phi}}^2 + \dot{\widehat{\theta}}^2\right) + \frac{1}{2}\left(\dot{\widehat{s}}^2 + \dot{\widehat{\bar{s}}}^2\right), \tag{3.8a}$$

where the dot denotes derivation w.r.t the JF cosmic time and the hatted fields read

$$\frac{d\widehat{\phi}}{d\phi} = \sqrt{K_{\Phi\Phi^*}} = J \simeq \frac{\sqrt{6(1+m)}}{x_\phi}, \quad \widehat{\theta} = J\,\theta x_\phi \ \text{ and } \ (\widehat{s}, \widehat{\bar{s}}) = \sqrt{K_{SS^*}}(s, \bar{s}). \tag{3.8b}$$

where $K_{SS^*} \simeq 1/c_{\mathcal{R}} x_\phi^2$ – cf. Eqs. (3.1b) and (3.1d). The spinors ψ_Φ and ψ_S associated with S and Φ are normalized similarly, i.e., $\widehat{\psi}_S = \sqrt{K_{SS^*}}\psi_S$ and $\widehat{\psi}_\Phi = \sqrt{K_{\Phi\Phi^*}}\psi_\Phi$. Integrating the first equation in Eq. (3.8b) we can identify the EF field:

$$\widehat{\phi} = \widehat{\phi}_{\rm c} + \sqrt{6(1+m)} m_{\rm P} \ln\frac{\phi}{\langle\phi\rangle} \ \text{ with } \ \langle\phi\rangle = \frac{\sqrt{2}m_{\rm P}}{\sqrt[n]{2c_{\mathcal{R}}}}, \tag{3.9}$$

where $\widehat{\phi}_{\rm c}$ is a constant of integration and we take into account Eqs. (2.1) and (2.4).

Upon diagonalization of $\widehat{M}_{\alpha\beta}^2$, we construct the mass spectrum of the theory along the path of Eq. (3.2). Taking advantage of the fact that $c_{\mathcal{R}} \gg 1$ and the limits $k_\Phi \to 0$ and $k_{S\Phi} \to 0$ we find the expressions of the relevant masses squared, arranged in Table 1, which approach rather well the quite lengthy, exact expressions taking into account in our numerical computation. In the limit $m = 0$ the expressions in Table R.1-1 are recovered. We have numerically verified that the various masses remain greater than $\widehat{H}_{\rm IG}$ during the last 50 e-foldings of inflation, and so any inflationary perturbations of the fields other than the inflaton are safely eliminated. They enter a phase of oscillations about zero with reducing amplitude and so the x_ϕ dependence in their normalization – see Eq. (3.8b) – does not affect their dynamics. As usually – cf. Ref. [1, 15] – the lighter eignestate of $\widehat{M}_{\alpha\beta}^2$ is $\widehat{m}_s^2$ which here can become positive and heavy enough for $k_S \gtrsim 0.1$ – see Sec. 3.4.

Inserting, finally, the mass spectrum of the model in the well-known Coleman-Weinberg formula, we calculate the one-loop corrected $\widehat{V}_{\rm IG}$

$$\widehat{V}_{\rm IG} = \widehat{V}_{\rm IG0} + \frac{1}{64\pi^2}\left(\widehat{m}_\theta^4 \ln\frac{\widehat{m}_\theta^2}{\Lambda^2} + 2\widehat{m}_s^4 \ln\frac{\widehat{m}_s^2}{\Lambda^2} - 4\widehat{m}_{\psi\pm}^4 \ln\frac{m_{\widehat{\psi}\pm}^2}{\Lambda^2}\right), \tag{3.10}$$

where Λ is a *renormalization group* (RG) mass scale. We determine it by requiring [21] $\Delta V(\phi_\star) = 0$ with $\Delta V = \widehat{V}_{\rm IG} - \widehat{V}_{\rm IG0}$. To reduce the possible [21] dependence of our results on the choice of Λ, we confine ourselves to λ and k_S values which do not enhance these corrections – see Sec. 3.4.

3.2 THE INFLATIONARY REQUIREMENTS

Based on $\widehat{V}_{\rm IG}$ in Eq. (3.10) we can proceed to the analysis of IG inflation in the EF [3], employing the standard slow-roll approximation [22]. We have just to convert the derivations and integrations w.r.t $\widehat{\phi}$ to the corresponding ones w.r.t ϕ keeping in mind the dependence of $\widehat{\phi}$ on ϕ, Eq. (3.8b). In particular, the observational requirements which are imposed on our inflationary scenario are outlined in the following.

3.2.1 The number of e-foldings, $\widehat{N}_\star$, that the scale $k_\star = 0.05/{\rm Mpc}$ suffers during IG inflation has to be adequate to resolve the horizon and flatness problems of standard big bang, i.e., [2, 23]

$$\widehat{N}_\star = \int_{\widehat{\phi}_{\rm f}}^{\widehat{\phi}_\star} \frac{d\widehat{\phi}}{m_{\rm P}^2}\frac{\widehat{V}_{\rm IG}}{\widehat{V}_{{\rm IG},\widehat{\phi}}} \simeq 19.4 + 2\ln\frac{\widehat{V}_{\rm IG}(\phi_\star)^{1/4}}{1\ {\rm GeV}} - \frac{4}{3}\ln\frac{\widehat{V}_{\rm IG}(\phi_{\rm f})^{1/4}}{1\ {\rm GeV}} + \frac{1}{3}\ln\frac{T_{\rm rh}}{1\ {\rm GeV}} + \frac{1}{2}\ln\frac{f_{\mathcal{R}}(\phi_{\rm f})}{f_{\mathcal{R}}(\phi_\star)^{1/3}}, \tag{3.11}$$

where $\phi_\star$ $[\widehat{\phi}_\star]$ is the value of ϕ $[\widehat{\phi}]$ when $k_\star$ crosses outside the inflationary horizon and $\phi_{\rm f}$ $[\widehat{\phi}_{\rm f}]$ is the value of ϕ $[\widehat{\phi}]$ at the end of IG inflation, which can be found from the condition

$$\max\{\widehat{\epsilon}(\phi_{\rm f}), |\widehat{\eta}(\phi_{\rm f})|\} = 1, \text{ where } \widehat{\epsilon} = \frac{m_{\rm P}^2}{2}\left(\frac{\widehat{V}_{{\rm IG},\widehat{\phi}}}{\widehat{V}_{\rm IG}}\right)^2 \text{ and } \widehat{\eta} = m_{\rm P}^2\,\frac{\widehat{V}_{{\rm IG},\widehat{\phi}\widehat{\phi}}}{\widehat{V}_{\rm IG}} \tag{3.12}$$

are the well-known slow-roll parameters and $T_{\rm rh}$ is the reheat temperature after IG inflation, which is taken $T_{\rm rh} = 10^9$ GeV throughout.

3.2.2 The amplitude $A_{\rm s}$ of the power spectrum of the curvature perturbation generated by ϕ at $k_\star$ has to be consistent with data [2]

$$\sqrt{A_{\rm s}} = \frac{1}{2\sqrt{3}\,\pi m_{\rm P}^3}\frac{\widehat{V}_{\rm IG}(\widehat{\phi}_\star)^{3/2}}{|\widehat{V}_{{\rm IG},\widehat{\phi}}(\widehat{\phi}_\star)|} = \frac{1}{2\pi m_{\rm P}^2}\sqrt{\frac{\widehat{V}_{\rm IG}(\phi_\star)}{6\widehat{\epsilon}_\star}} \simeq 4.685\cdot 10^{-5}, \tag{3.13}$$

where the variables with subscript $\star$ are evaluated at $\phi = \phi_\star$

3.2.3 The remaining inflationary observables $n_{\rm s}, a_{\rm s}$ and r – estimated through the relations:

$$\text{(a) } n_{\rm s} = 1 - 6\widehat{\epsilon}_\star + 2\widehat{\eta}_\star, \quad \text{(b) } a_{\rm s} = 2\left(4\widehat{\eta}_\star^2 - (n_{\rm s}-1)^2\right)/3 - 2\widehat{\xi}_\star \text{ and } \text{(c) } r = 16\widehat{\epsilon}_\star, \tag{3.14}$$

with $\widehat{\xi} = m_{\rm P}^4\widehat{V}_{{\rm IG},\widehat{\phi}}\widehat{V}_{{\rm IG},\widehat{\phi}\widehat{\phi}\widehat{\phi}}/\widehat{V}_{\rm IG}^2$ – have to be consistent with the data [2], i.e.,

$$\text{(a) } n_{\rm s} = 0.96 \pm 0.014, \quad \text{(b) } -0.0314 \leq a_{\rm s} \leq 0.0046 \text{ and } \text{(c) } r \leq 0.135 \text{ at } 95\% \text{ c.l.}, \tag{3.15}$$

pertaining to the ΛCDM framework. The last inequality can be complimented by the BICEP2 data as shown in Eq. (1.1).

3.2.4. Since SUGRA is an effective theory below $m_{\rm P}$ the existence of higher-order terms in W and K, Eqs. (2.1) and (2.13), appears to be unavoidable. Therefore the stability of our inflationary solutions can be assured if we entail

$$\text{(a) } \widehat{V}_{\rm IG}(\phi_\star)^{1/4} \leq m_{\rm P} \text{ and } \text{(b) } \phi_\star \leq m_{\rm P}, \tag{3.16}$$

where $m_{\rm P}$ is the UV cutoff scale of the effective theory for the present models, as shown in Sec. 4.

3.3 ANALYTIC RESULTS

Plugging Eqs. (3.5) and (3.8b) into Eq. (3.12) and taking $k_\Phi \simeq 0$, we obtain the following approximate expressions for the slow-roll parameters

$$\begin{aligned}\widehat{\epsilon} &= \frac{(2+3m-3mc_{\mathcal{R}}x_\phi^2+(1+3m)k_{S\Phi}c_{\mathcal{R}}x_\phi^4)^2}{3(1+m)f_{S\Phi}^2f_2^2} \quad \text{and} \quad \widehat{\eta}=\frac{1}{3(1+m)f_{S\Phi}^2f_2^2}\times\\ \times &\quad 2\Big[x_\phi^2\Big(k_{S\Phi}\left(x_\phi^2\left(6c_{\mathcal{R}}+c_{\mathcal{R}}^2x_\phi^2+k_{S\Phi}c_{\mathcal{R}}^2x_\phi^4\right)-11\right)-2c_{\mathcal{R}}\Big)+9m^2f_{S\Phi}^2f_2^2\\ + &\quad 4+6mf_{S\Phi}f_2\left(2+k_{S\Phi}x_\phi^2(c_{\mathcal{R}}x_\phi^2-3)\right)\Big]\,. \end{aligned} \tag{3.17}$$

Taking the limit of the expressions above for $k_{S\Phi}\simeq 0$ we can analytically solve the condition in Eq. (3.12) w.r.t x_ϕ. The results are

$$\frac{\phi_{1\rm f}}{m_{\rm P}}=\sqrt{\frac{3(1-m)+2\sqrt{3(1+m)}}{3(1+m)c_{\mathcal{R}}}} \quad \text{and} \quad \frac{\phi_{2\rm f}}{m_{\rm P}}=\sqrt{\frac{1-9m+\sqrt{16+21m(3m-1)}}{3(1+m)c_{\mathcal{R}}}}\cdot \tag{3.18}$$

The end of IG inflation mostly occurs at $\phi_{\rm f}=\phi_{1\rm f}$ because this is mainly the maximal value of the two solutions above.

Since $\phi_{\rm f}\ll\phi_\star$, we can estimate $\widehat{N}_\star$ through Eq. (3.11) neglecting $\phi_{\rm f}$. Our result is

$$\widehat{N}_\star\simeq(1+m)\frac{3m\ln x_\star+\ln\left(2+3m-3c_{\mathcal{R}}mx_\star^2\right)}{|m|(2+3m)} \quad \text{with} \quad x_\star=\phi_\star/m_{\rm P}\cdot \tag{3.19a}$$

Ignoring the first term in the last equality and solving w.r.t $x_\star$ we extract $\phi_\star$ as follows

$$\phi_\star\simeq m_{\rm P}/\sqrt{3|m|c_{\mathcal{R}}e_m} \quad \text{with} \quad e_m=e^{m(2+3m)\widehat{N}_\star/(1+m)} \tag{3.19b}$$

Although a radically different dependence of $\phi_\star$ on $\widehat{N}_\star$ arises compared to the models of Ref. [1] – cf. Eq. (R.1-3.17a) – $\phi_\star$ can again remain subplanckian for large $c_{\mathcal{R}}$'s. Indeed,

$$\phi_\star\leq m_{\rm P} \quad\Rightarrow\quad c_{\mathcal{R}}\geq 1/3|m|e_m\,. \tag{3.19c}$$

As emphasized in Ref. [1], this achievement is crucial for the viability of our proposal, since it protects the inflationary computation against higher-order corrections from non-renormalizable terms in $\Omega_{\rm H}$ – see Eq. (2.1). Note that $\Omega_{\rm H}$ is totally defined in terms of Φ. In other words, our setting is independent of $\widehat{\phi}_\star$ which can be found by Eq. (3.9) and remains transplanckian. Indeed, plugging Eq. (3.19b) into Eq. (3.9) we find

$$\widehat{\phi}_\star\simeq\widehat{\phi}_{\rm c}-m_{\rm P}\sqrt{3(1+m)/2}\left(\ln 3|m|+m(2+3m)\widehat{N}_\star/(1+m)\right), \tag{3.20}$$

which yields $\widehat{\phi}_\star\simeq(8.9-12)m_{\rm P}$ for $\widehat{\phi}_{\rm c}=0$ and $m=-(0.04-0.0625)$. Interestingly enough, $\widehat{\phi}_\star$ turns out to be independent of $c_{\mathcal{R}}$ – as the result shown in Eq. (R.1-3.18). Note that the independence of $k_{S\Phi}$ is artificial since we ignore $k_{S\Phi}$ in the estimations below Eq. (3.18).

Upon substitution of Eq. (3.19b) into Eq. (3.13) we end up with

$$A_{\rm s}^{1/2}\simeq\frac{\lambda c_{\mathcal{R}}^{-3m/2}x_\star^{2-3m}}{4\sqrt{2}\pi(2-3c_{\mathcal{R}}mx_\star^2+k_{S\Phi}c_{\mathcal{R}}x_\star^4)} \;\Rightarrow\; \lambda\simeq\frac{4\pi\sqrt{2A_{\rm s}}\left(k_{S\Phi}+9c_{\mathcal{R}}m^2e_m(1+2e_m)\right)}{3^{1+3m/2}(|m|e_m)^{1+3m/2}}\cdot \tag{3.21}$$

We remark that λ remains proportional to $c_{\mathcal{R}}$ as for the other models of Ref. [1] – cf. Eqs. (R.1-3.19) and (R.1-3.29) – but it depends also on both $k_{S\Phi}$ and m. Inserting Eq. (3.19b) into Eq. (3.17), employing then Eq. (3.14a) and expanding for $c_{\mathcal{R}}\gg 1$ we find

$$n_{\rm s}\simeq 1-2m\frac{3m(1+4e_m)-4e_m(1-3me_m)}{1+m}-4k_{S\Phi}\frac{1+3m(1+10e_m)-36m^2e_m}{9c_{\mathcal{R}}m(1+m)e_m}\cdot \tag{3.22a}$$

INPUT PARAMETERS												
$-m/10^{-2}$	4		5		6		4		5		6	
$c_{\mathcal{R}}/10^3$	1.9	5.3	5.59	9	17.7	35.5	1.9	5.3	5.59	9	17.7	35.5
$-k_{S\Phi}/10^{-2}$	1.1	3	2	3.2	2.9	6	1.1	3	2	3.2	2.9	6
OUTPUT PARAMETERS												
	ANALYTIC RESULTS						NUMERICAL RESULTS					
$\lambda/0.1$	1.3	3.5	4	6.5	1.3	26	1.1	3.2	3.3	5.3	9.7	19
$\phi_\star/m_{\rm P}$	0.57	0.34	0.5	0.4	0.43	0.3	1	0.6	1	0.8	1	0.7
$\widehat{\phi}_\star/m_{\rm P}$	7.7		8.65		9.62		9		10.3		11.6	
$\phi_{\rm f}/0.01m_{\rm P}$	3.4	2	2	1.6	1	0.8	3.4	2	2	1.6	1	0.8
$\widehat{N}_\star$	56	57	56	56.5	56.3	56.8	55.5	55.6	56.4	56.7	56.9	56.9
$n_{\rm s}$	0.98		0.976		0.97		0.975		0.96		0.946	
r	0.08		0.12		0.17		0.07		0.09		0.13	
$\widehat{m}_\theta^2/\widehat{H}_{\rm IG}^2\,(\phi_\star)$	3.92	3.96	3.97	3.97	3.98		3.9		3.9		3.9	
$\widehat{m}_s^2/\widehat{H}_{\rm IG}^2\,(\phi_{\rm f})$	2.64	2.64	2.75	2.75	2.9		3.64		3.65		3.67	

Table 2: *Comparison between the analytic and numerical results for six different sets of input and output parameters of our model. We take $k_S = 0.1$, $k_\Phi = 0.5$ and $T_{\rm rh} = 10^9$ GeV. Our numerical results are consistent with Eqs. (1.1), (3.11), (3.13), (3.15) and (3.16).*

From this expression we see that $m < 0$ and $k_{S\Phi} < 0$ assist us to reduce $n_{\rm s}$ sizably lower than unity as required in Eq. (3.15a). Making use of Eqs. (3.19b), (3.17) and (3.14c) we arrive at

$$r \simeq \frac{48m^2(1+2e_m)^2}{(1+m)(1+3me_m)^2} + \frac{32k_{S\Phi}(1+2e_m)(1-6me_m)}{3c_{\mathcal{R}}e_m(1+m)(1+3me_m)^2}. \tag{3.22b}$$

From the last result we conclude that primarily $|m| \neq 0$ and secondary $m < 0$ help us to increase r.

To appreciate the validity of our analytic estimates, we test them against our numerical ones. The relevant results are displayed in Table 2. We use six sets of input parameters – see also Sec. 3.4 – and we present their response by applying the formulae of Sec. 3.3 (first six columns to the right of the leftmost one) or using the formulae of Sec. 3.2 with $\widehat{V}_{\rm IG}$ given in Eq. (3.10) (next six columns). We see that the results are quite close to each other with an exception regarding $\phi_\star$ whose the numerical and analytic values appreciably differ. This fact can be attributed to the inaccuracy of Eq. (3.19b) whose the derivation is based on a number of efficient simplifications. Despite this deviation, the absence of $\phi_{\rm f}$ from Eq. (3.19a) assists us to evaluate rather accurately $\widehat{N}_\star$ and the analytic values of $\widehat{\phi}_\star$, r and $n_{\rm s}$ are rather close to the numerical ones. As anticipated in Eq. (3.20), $\widehat{\phi}_\star$ is independent of $c_{\mathcal{R}}$ (and $k_{S\Phi}$). Finally, from the two last rows of Table 2 we see that the formulas of Table 1 are reliable enough. As can be deduced by the relevant expressions, $\widehat{m}_s^2$ is a monotonically increasing function of x_ϕ and so its minimal value is encountered for $\phi = \phi_{\rm f}$. On the contrary, the minimal $\widehat{m}_\theta^2$ is located at $\phi = \phi_\star$.

It is clear that the $n_{\rm s}$ and r values obtained in Table 2 are perfectly consistent with both the *Planck* and BICEP2 results – cf. Eqs. (1.1) and (3.14a,b). Furthermore, the resulting r remains constant for constant m and $n_{\rm s}$ and is independent on λ (or $c_{\mathcal{R}}$). This feature is verified by our analytical estimate in Eq. (3.22b) from which we observe that the dominant contribution originates from the first fraction, which is independent of $k_{S\Phi}$ and $c_{\mathcal{R}}$, whereas the correction of the second fraction is

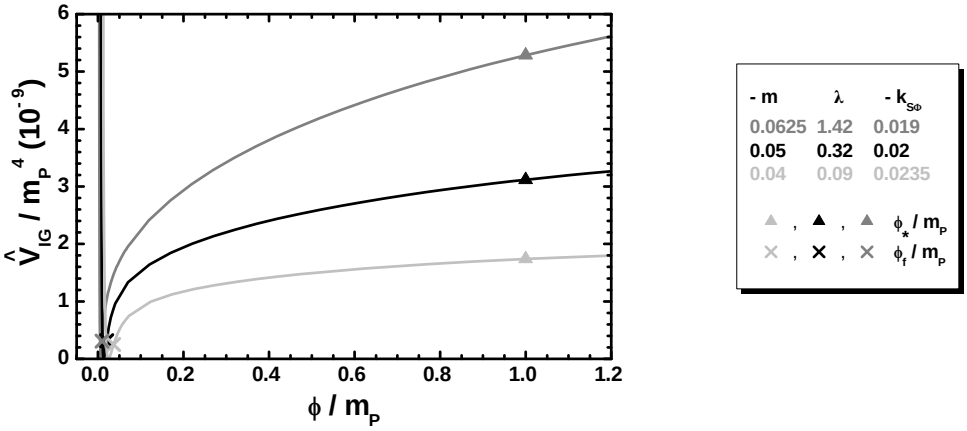

Figure 1: *The inflationary potential $\widehat{V}_{\rm IG}$ as a function of ϕ for $n = 2$. The light gray, black and gray line is obtained by setting $-m = 0.04, 0.05, 0.0625$, $\lambda = 0.09, 0.32, 1.42$ and $-k_{S\Phi} \simeq 0.0235, 0.02, 0.019$ respectively. The values corresponding to $\phi_\star$ and $\phi_{\rm f}$ are also depicted.*

suppressed by the inverse power of $c_{\mathcal{R}}$. The most impressive point, however, is that these large r values are accommodated with subplanckian values of ϕ. As first stressed in Ref. [23], this fact does not contradict to the Lyth bound [24], since the latter bound is applied to the EF canonically normalized inflaton field $\widehat{\phi}$ which remains transplanckian and close to the value shown in Eq. (3.20). Therefore, large r's do not necessarily [25] correlate with transplanckian excursions of ϕ within IG inflation.

3.4 NUMERICAL RESULTS

As shown in Eqs. (2.1), (2.13) and (3.11), this inflationary scenario depends on the parameters:

$$\lambda,\ c_{\mathcal{R}},\ m,\ k_S,\ k_{S\Phi},\ k_\Phi \ \text{ and } \ T_{\rm rh}.$$

Besides the free parameters employed in Sec. R.1-3.3.3, we here have m which is constrained to negative values in order to ensure the boundedness from below of $\widehat{V}_{\rm IG0}$ – see Eq. (3.5). Using the reasoning of Sec. R.1-3.3.3, we set $k_\Phi = 0.5$ and $T_{\rm rh} = 10^9$ GeV. On the other hand, $\widehat{m}_s^2$ becomes positive with k_S's lower than those used in Sec. R.1-3.3.3 since positive contributions from $m < 0$ arise here – see in Table 1. Moreover, due to the relatively large λ's encountered in our scheme, if k_S takes a value of order unity $\widehat{m}_s^2$ grows more efficiently than in the cases with $m = 0$, rendering thereby the radiative corrections in Eq. (3.10) sizeable for very large $c_{\mathcal{R}}$'s. To avoid such a certainly unpleasant dependence of the model predictions on the radiative corrections we tune somehow k_S to lower values than those used in Sec. R.1-3.3.3. E.g. we set $k_S = 0.1$ throughout. For the same reason we confine ourselves to the lowest possible n, $n = 2$. Eqs. (3.11), (3.13) and (3.16) assist us to restrict λ (or $c_{\mathcal{R}} \geq 1$) and $\phi_\star$. By adjusting m and $k_{S\Phi}$ we can achieve not only $n_{\rm s}$'s in the range of Eq. (3.15a) but also r's in the optimistic region of Eq. (1.1).

The structure of $\widehat{V}_{\rm IG}$ as a function of ϕ for $m < 0$ (and $n = 2$) is visualized in Fig. 1, where we depict $\widehat{V}_{\rm IG}$ versus ϕ for $\phi_\star = m_{\rm P}$ and the selected values of $\lambda, k_{S\Phi}$ and m, shown in the label. These choices require that $c_{\mathcal{R}}$'s are $(1.7, 5.6, 26) \cdot 10^3$ and result to $n_{\rm s} = 0.96$ and $r = 0.053, 0.096, 0.16$ for increasing $|m|$'s – light gray, black and gray line correspondingly. It would be instructive to compare Fig. 1 with Fig. R.1-1, where $\widehat{V}_{\rm IG}$ for $m = 0$ is displayed – the fact that we employ a vanishing $k_{S\Phi}$ in Fig. R.1-1 does not invalidate the comparison since the impact of $k_{S\Phi}$ on the form of $\widehat{V}_{\rm IG}$ is almost invisible. We remark that in Fig. 1

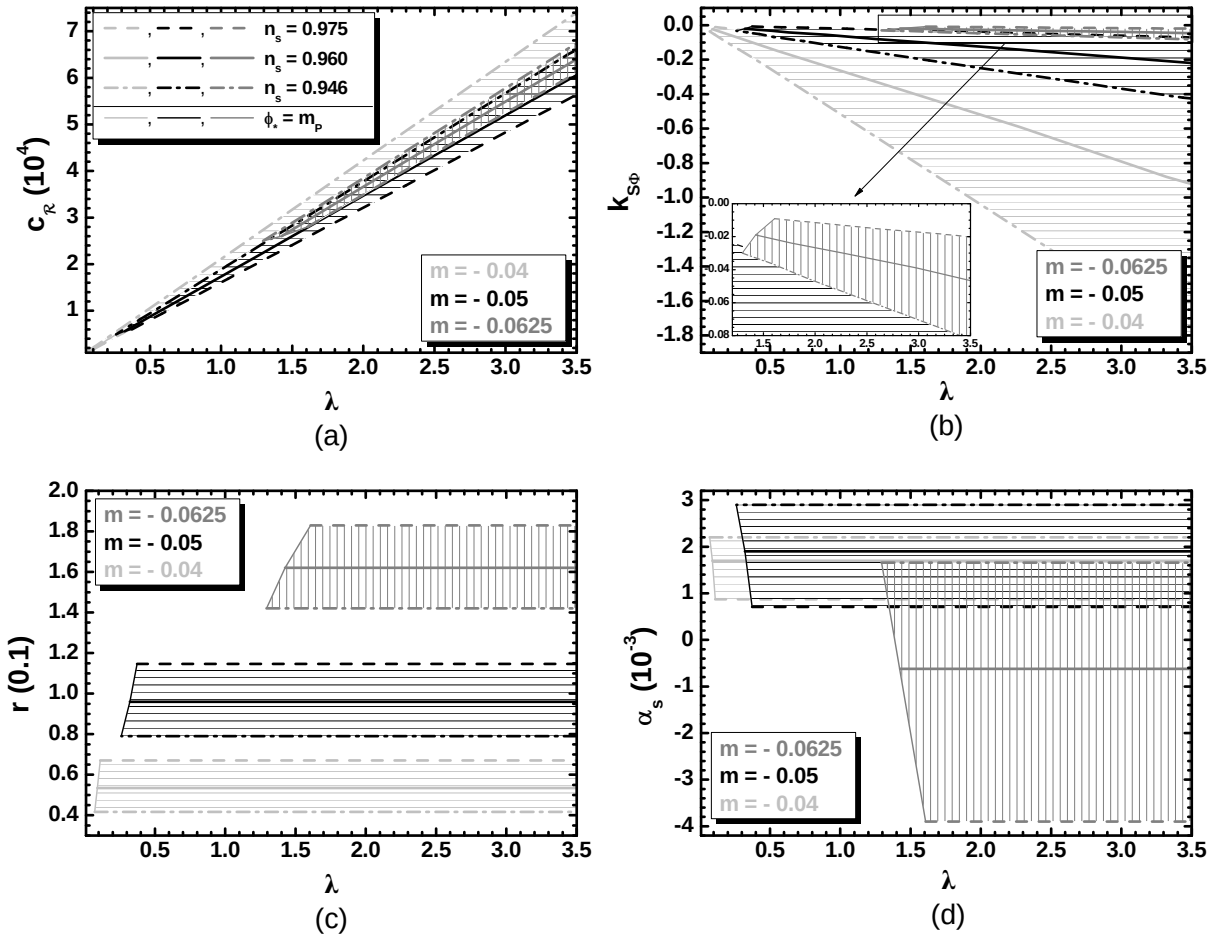

Figure 2: *The (hatched) regions allowed by Eqs. (3.11), (3.13), (3.15*a, b*) and (3.16) in the $\lambda - c_{\mathcal{R}}$ (*a*), $\lambda - k_{S\Phi}$ (*b*), $\lambda - r$ (*c*), $\lambda - a_{\rm s}$ (*d*) plane for $n = 2$, $k_S = 0.1$, $k_\Phi = 0.5$ and $m = -0.04$ (light gray lines and hatched regions), $m = -0.05$ (black lines and hatched regions) $m = -0.0625$ (gray lines and hatched regions). The conventions adopted for the type and color of the various lines are also shown in the label of panel* (a).

(i) The values of $\widehat{V}_{\rm IG0}$ for $\phi = \phi_\star$ are one order of magnitude larger than those encountered in Fig. R.1-1; actually $\widehat{V}^{1/4}_{\rm IG0}$ approaches the SUSY grand-unification scale, $2 \cdot 10^{16}$ GeV, which is imperative – see, e.g., Ref. [25] – for achieving r values of order 0.1;

(ii) $\widehat{V}_{\rm IG0}$ close to $\phi = \phi_\star$ acquires a steeper slope which increases with $|m|$ and results to an enhancement of $\widehat{\epsilon}_\star$ – see Eq. (3.17) – and, via Eq. (3.14c), of r.

Another difference of the present set-up regarding those of Ref. [1] is that for $m = 0$ we obtain constantly $\eta_\star < 0$ whereas we here obtain $\eta_\star > 0$ for $n_{\rm s} > 0.97$ and $\eta_\star < 0$ for lower $n_{\rm s}$ values.

Confronting the models under consideration with the constraints of Eqs. (3.11), (3.13), (3.15a, b) and (3.16) we depict the allowed (hatched) regions in the $\lambda - c_{\mathcal{R}}$, $\lambda - k_{S\Phi}$, $\lambda - r$ and $\lambda - a_{\rm s}$ plane for $m = -0.04$ (light gray lines and horizontally hatched regions), $m = -0.05$ (black lines and horizontally hatched regions), $m = -0.0625$ (gray lines and vertically hatched regions) – see Fig. 2-(a), (b), (c) and (d) respectively. In the horizontally hatched regions r is compatible with Eq. (1.1) whereas in the vertically hatched region r turns out to be close to the central value suggested [4] by BICEP2 – after subtraction of a dust foreground. The conventions adopted for the various lines are also

shown in the label of panel (a). In particular, the dashed [dot-dashed] lines correspond to $n_{\rm s}=0.975$ [$n_{\rm s}=0.946$], whereas the solid (thick) lines are obtained by fixing $n_{\rm s}=0.96$ – see Eq. (3.15a). The lower bound for the regions presented in Fig. 2 is provided by the constraint of Eq. (3.16b) which is saturated along the thin lines. The perturbative bound on λ limits the various regions at the other end.

From Fig. 2-(a) we remark that $c_{\mathcal{R}}$ remains almost proportional to λ but the dependence on $k_{S\Phi}$ is stronger than that shown in Fig. R.1-2–(a_1) and (a_2). Also as $|m|$ increases, the allowed areas become smaller favoring larger $c_{\mathcal{R}}$'s and λ's. From Fig. 2-(b) we notice that the allowed $k_{S\Phi}$'s get concentrated around zero as $|m|$ increases and so the relevant tuning increases. Finally from Fig. 2-(c) and (d) we conclude that decreasing m below zero, r and $a_{\rm s}$ increase w.r.t their standard values – cf. Eq. (R.1-3.22) and discussion below Eq. (R.1-3.32c). As a consequence, r for $m=-0.04$ and -0.05 approaches the range of Eq. (1.1) – which explains (conservatively) the recent BICEP2 results – being at the same time compatible with the *Planck* (and WMAP) measurements. For $m=-0.0625$, r reaches its (almost) maximal possible value in our set-up which lie close to the BICEP2 central r value – see Sec. 1 above Eq. (1.1). On the other hand, $a_{\rm s}$ remains sufficiently low; it is thus consistent with the fitting of data with the standard ΛCDM model – see Eq. (R.1-3.6b). Namely, $|a_{\rm s}|$ never exceeds $4\cdot 10^{-3}$ and it is mostly positive. It is clear, therefore, that it is much smaller than its best-fit value of roughly -0.02 which may help [4, 26] to relieve the tension between the BICEP2 and the *Planck* data as regards the bounds on r. Furthermore, the resulting $a_{\rm s}$ follows the behavior of r, which depends only on the input m and $k_{S\Phi}$ (or $n_{\rm s}$) and are independent on λ (or $c_{\mathcal{R}}$) – as anticipated in the end of Sec. 3.3. More explicitly, for $n_{\rm s}=0.96$ and $\widehat{N}_\star\simeq 55-57$ we find:

$$0.17\lesssim\frac{c_{\mathcal{R}}}{10^4}\lesssim 6.7\ \ \text{with}\ \ 0.09\lesssim\lambda\lesssim 3.5\ \ \text{and}\ \ 0.2\lesssim-\frac{k_{S\Phi}}{0.1}\lesssim 9.3\ \ (m=-0.04);\tag{3.23a}$$

$$0.56\lesssim\frac{c_{\mathcal{R}}}{10^4}\lesssim 6.1\ \ \text{with}\ \ 0.32\lesssim\lambda\lesssim 3.5\ \ \text{and}\ \ 0.02\lesssim-\frac{k_{S\Phi}}{0.1}\lesssim 2.2\ \ (m=-0.05);\tag{3.23b}$$

$$2.6\lesssim\frac{c_{\mathcal{R}}}{10^4}\lesssim 6.45\ \ \text{with}\ \ 1.4\lesssim\lambda\lesssim 3.5\ \ \text{and}\ \ 1.9\lesssim-\frac{k_{S\Phi}}{0.01}\lesssim 4.7\ \ (m=-0.0625).\tag{3.23c}$$

In these regions we obtain

$$\frac{r}{0.1}=0.53,0.96,1.6\ \ \text{and}\ \ \frac{a_{\rm s}}{0.001}=1.7,1.9,-0.6\ \ \text{for}\ \ -\frac{m}{0.01}=4,5,6.25\tag{3.24}$$

respectively. Consequently, our model can fit both *Planck* and BICEP2 results adjusting just two more parameters (m and $k_{S\Phi}$) than those employed in the initial (and more robust) model [1] exhibiting the no-scale-type symmetry.

It is worth noticing that a decrease of $k_{S\Phi}$ below zero is imperative in order to achieve a simultaneous fulfillment of Eq. (3.15a) and (1.1). Indeed, selecting $k_{S\Phi}=0$ the increase of the prefactor (-3) in K generates an enhancement of r which is accompanied by an increase of $n_{\rm s}$ beyond the range of Eq. (3.15a). Therefore, the new solutions to the tachyonic instability problem which avoid terms of the form $|S|^2|\Phi|^2$ in K [18–20] are expected not to fit well with our proposal. Increasing, finally, n above 2 the required λ and $c_{\mathcal{R}}$ values become larger and so the allowed regions are considerably shrunk; we thus do not pursue further our investigation.

In closing, it would be instructive to compare our proposal with the so-called α-attractor models [12] where deviations from the conventional (-3) coefficient of the logarithm in the Kähler potential are also investigated. Namely, focusing in Sec. 7.2 of the second paper in Ref. [12] we can remark the following essential differences:

(i) In the Kähler potential the inflaton appears linearly, and not quadratically as in our case, without a large coefficient $c_{\mathcal{R}}$ and no terms exist proportional to $k_{S\Phi}$ and k_Φ. Therefore, no dependence on those parameters is studied. Moreover no restrictions from IG are taken into account.

(ii) The numerical prefactor of the logarithm in the Kähler potential appears also in the exponent of the superpotential in a such way that the inflationary potential, derived from Eq. (3.1a), has no dependence on $\alpha = 1+m$ besides the one involved in expressing the JF inflaton T in terms of EF one φ. The inflationary potential depends only on an *arbitrary* exponent called n which enters the definition of the function $\tilde{f}$ in Eq. (7.12). In an explicit example mentioned in the last paragraph of Sec. 7.2 the form $\tilde{f} = T - 1$ is adopted and the inflationary potential has the simplest form $V_0(1 - e^{-\sqrt{2/3\alpha}\varphi/m_{\rm P}})^2$.

As a consequence of the arrangements above, the models of Ref. [12] asymptote to Starobinsky model for low α's and to quadratic inflation for very large α's – obviously, trasplanckian values for T and φ are employed. This behavior is not observed in our setting. The reason can be transparently shown if we express $\widehat{V}_{\rm IG0}$ in Eq. (3.5) in terms of $\widehat{\phi}$ defined in Eq. (3.9) – with $\widehat{\phi}_{\rm c} = 0$ – as follows:

$$\widehat{V}_{\rm IG0} \simeq \frac{\lambda^2 m_{\rm P}^4}{4 f_{S\Phi} c_{\mathcal{R}}^2} e^{-\sqrt{6/(1+m)}m\widehat{\phi}/m_{\rm P}} \left(1 - e^{-\sqrt{2/3(1+m)}\widehat{\phi}/m_{\rm P}}\right)^2 , \tag{3.25}$$

where we assumed $f_{\phi\phi} \simeq 1$ and the last factor originates from the quantity $f_2^2/c_{\mathcal{R}}^2 x_\phi^4$ – with f_2 defined below Eq. (3.4). From the last expression we can easily infer that, for $m \neq 0$, $\widehat{V}_{\rm IG0}$ declines away from the simplest form found in Ref. [12]. Indeed, in our set-up the last factor of Eq. (3.25), which already exists in Ref. [12], is multiplied by $x_\phi^{-6m}/f_{S\Phi} c_{\mathcal{R}}^{3m} = e^{-\sqrt{6/(1+m)}m\widehat{\phi}/m_{\rm P}}/f_{S\Phi}$. This last factor has a significant impact on our results – see Eq. (3.22b).

4 THE EFFECTIVE CUT-OFF SCALE

The realization of IG inflation with $m < 0$ retains the perturbative unitarity up to $m_{\rm P}$ as the models described in Ref. [1] do – cf. Ref. [15, 16]. Focusing first on the JF computation, we remark that the argument goes as analyzed in Sec. R.1-4.1 with $F_{\rm K}$ taking the form

$$F_{\rm K} \simeq 1 - \frac{nm}{(1+m)} + \frac{3}{2x_\phi^2}\, mn^2 \Omega_{\rm H} \;\Rightarrow\; \langle F_{\rm K}\rangle \simeq 1 - \frac{nm}{(1+m)} + \frac{3}{8} 2^{2/n}\, mn^2 c_{\mathcal{R}}^{2/n}, \tag{4.1}$$

as can be easily inferred from the second term of Eq. (2.10). The last expression in Eq. (4.1) can be extracted taking into account Eqs. (2.4) and (3.9). Here, and henceforth, we keep the dependence of the formulas on the exponent n for better comparison with the formulas in Sec. R.1-4. Inserting Eq. (4.1) into Eq. (R.1-4.3) we can conclude that UV cut-off scale $\Lambda_{\rm UV}$ is still roughly equal to $m_{\rm P}$ since the dangerous prefactor $c_{\mathcal{R}}^{-2/n}$ is eliminated. Needless to say, terms proportional to $k_{S\Phi}$ or k_Φ included in Eq. (2.13) are small enough and do not generate any problem with the perturbative unitarity. Therefore, they do not influence our conclusions.

Moving on to the EF, recall – see Eqs. (3.8b) and (3.9) – that the canonically normalized inflaton,

$$\widehat{\delta\phi} = \langle J\rangle \delta\phi \;\; \text{with} \;\; \langle J\rangle \simeq \sqrt{\frac{3(1+m)}{2}} \frac{n}{\langle x_\phi\rangle} = \frac{\sqrt{3}}{2}\, n \sqrt[n]{2c_{\mathcal{R}}} \tag{4.2}$$

acquires mass which is calculated to be

$$\widehat{m}_{\delta\phi} = \left\langle \widehat{V}_{{\rm IG0},\widehat{\phi}\widehat{\phi}} \right\rangle^{1/2} \simeq \lambda m_{\rm P}/\sqrt{3(1+m)} c_{\mathcal{R}}\,. \tag{4.3}$$

We remark that $\widehat{m}_{\delta\phi}$ turns out to be largely independent of n as in Eq. (R.1-4.5). However, due to the modified $\lambda - c_{\mathcal{R}}$ relation – see Eq. (3.21) – and the factor $\sqrt{1+m} < 1$ in the denominator, its numerical value increases slightly w.r.t its value in the models of Ref. [1]. E.g., taking $\phi_\star = 0.6 m_{\rm P}$

and $m = -(0.04 - 0.625)$ we get $6.9 \lesssim \widehat{m}_{\delta\phi}/10^{13}$ GeV $\lesssim 9.2$ for $n_{\rm s}$ in the range of Eq. (R.1-3.6a). Since we do not find any attractor towards the quadratic inflation, $\widehat{m}_{\delta\phi}$ is clearly disguisable from its value encountered in that model.

To check the limit of the validity of the effective theory, we expand $J^2\dot{\phi}^2$ involved in Eq. (2.6) about $\langle\phi\rangle$ in terms of $\widehat{\delta\phi}$ in Eq. (4.2) and we arrive at the following result

$$J^2\dot{\phi}^2 = \left(1 - \frac{2(1+2m+m^2)}{n(1+m)^{5/2}}\sqrt{\frac{2}{3}}\frac{\widehat{\delta\phi}}{m_{\rm P}} + \frac{2}{n^2(1+m)}\frac{\widehat{\delta\phi}^2}{m_{\rm P}^2} - \frac{8}{3n^3(1+m)^{3/2}}\sqrt{\frac{2}{3}}\frac{\widehat{\delta\phi}^3}{m_{\rm P}^3} + \cdots\right)\dot{\widehat{\delta\phi}}^2. \tag{4.4}$$

The expansion corresponding to $\widehat{V}_{\rm IG0}$ in Eq. (3.4) with $k_{S\Phi} \simeq 0$ and $k_\Phi \simeq 0$ includes the terms – cf. Eq. (R.1-4.6c):

$$\widehat{V}_{\rm IG0} = \frac{\lambda^2 m_{\rm P}^2\widehat{\delta\phi}^2}{6c_{\mathcal{R}}^2(1+m)} \cdot \left[1 - \sqrt{\frac{2}{3}}\left(1 + \frac{1}{n} + m\left(4 + 3m + \frac{1}{n}\right)\right)\frac{\widehat{\delta\phi}}{(1+m)^{3/2}m_{\rm P}} + \left(\frac{7}{18} + \frac{1}{n} + \frac{11}{18n^2} + m\left(2 + 3m + \frac{3}{n}\right)\right)\frac{\widehat{\delta\phi}^2}{(1+m)m_{\rm P}^2} - \cdots\right]. \tag{4.5}$$

Hence, we can conclude from Eqs. (4.4) and (4.5) that in this case also $\Lambda_{\rm UV} = m_{\rm P}$, in agreement with our analysis in the JF.

5 CONCLUSIONS

Prompted by the recent excitement – see e.g. Ref. [10–12] – in the are(n)a of inflationary model building, we carried out a confrontation of IG inflation, formulated beyond the no-scale SUGRA, with the *Planck* [2] and BICEP2 results [4] – regardless of the ongoing debate on the ultimate validity of the latter [7,8]. As in our original paper, Ref. [1], the inflationary models are tied to a superpotential, which realizes easily the idea of IG, and a logarithmic Kähler potential, which includes all the allowed terms up to the fourth order in powers of the various fields – see Eq. (2.13). The models are totally defined imposing two global symmetries – a continuous R and a discrete $\mathbb{Z}_n$ symmetry – in conjunction with the requirement that the original inflaton takes subplanckian values. Extending our work in Ref. [1] we allow for deviations from the prefactor (-3) multiplying the logarithm of the Kähler potential– see Eq. (2.13). We parameterized these deviation by a factor $(1+m)$. Fixing $n = 2$, confining m to the range $-(4 - 6.25)\%$ and adjusting $\lambda,\ c_{\mathcal{R}}$ and $(-k_{S\Phi})$ in the ranges $0.09 - 3.5$, $(1.7 - 64.5)\cdot 10^3$ and $0.019 - 0.93$ correspondingly, we achieved inflationary solutions that are simultaneously *Planck* and BICEP2-friendly, i.e. we obtained $n_{\rm s} \simeq 0.96$ and $0.05 \lesssim r \lesssim 0.16$ with negligible small $a_{\rm s}$. A mild tuning of k_S to values of order 0.1 is adequate such that the one-loop radiative corrections remain subdominant. Moreover, the corresponding effective theory remains trustable up to $m_{\rm P}$, as in the other cases analyzed in Ref. [1]. As a bottom line we could say that although incarnations of IG inflation beyond the no-scale SUGRA are less predictive than the simplest model presented in Ref. [1] they provide us with the adequate flexibility needed to obtain larger r's without disturbing the remaining attractive features of this inflationary model.

ACKNOWLEDGEMENTS

This research was supported from the Generalitat Valenciana under contract PROMETEOII/2013/017. I would like to acknowledge useful discussions with G. Lazarides and dedicate this paper to the memory of my High School Greek language teacher V. Aspiotis, a friend and a mentor with a valuable impact on my culture.

REFERENCES

[1] C. Pallis, *J. Cosmol. Astropart. Phys.* **08**, 057 (2014) [arXiv:1403.5486].

[2] P.A.R. Ade *et al.* [*Planck* Collaboration], arXiv:1303.5082.

[3] A. Zee, *Phys. Rev. Lett.* **42**, 417 (1979);
D. S. Salopek, J. R. Bond and J.M. Bardeen, *Phys. Rev. D* **40**, 1753 (1989);
R. Fakir and W.G. Unruh, *Phys. Rev. D* **41**, 1792 (1990).

[4] P.A.R. Ade *et al.* [BICEP2 Collaboration], *Phys. Rev. Lett.* **112**, 241101 2014) [arXiv:1403.3985].

[5] G.F. Giudice and H.M. Lee, *Phys. Lett. B* **733**, 58 (2014) [arXiv:1402.2129].

[6] R. Kallosh, arXiv:1402.3286;
R. Kallosh, A. Linde and D. Roest, arXiv:1407.4471;
B. Mosk and J. P. van der Schaar, arXiv:1407.4686.

[7] H. Liu, P. Mertsch and S. Sarkar, arXiv:1404.1899.

[8] M.J. Mortonson and U. Seljak, arXiv:1405.5857;
R. Flauger, J.C. Hill and D.N. Spergel, arXiv:1405.7351.

[9] R. Adam *et al.* [*Planck* Collaboration], arXiv:1409.5738;
M. Cortês, A.R. Liddle and D. Parkinson, arXiv:1409.6530;
C. Cheng, Q.G. Huang and S. Wang, arXiv:1409.7025.

[10] S. Ferrara, A. Kehagias and A. Riotto, arXiv:1403.5531;
R. Kallosh, A. Linde, B. Vercnocke and W. Chemissany, arXiv:1403.7189;
K. Hamaguchi, T. Moroi and T. Terada, *Phys. Lett. B* **733**, 305 (2014) [arXiv:1403.7521];
A.B. Lahanas and K. Tamvakis, arXiv:1405.0828;
G.K. Chakravarty and S. Mohanty, arXiv:1405.1321;
S. Ferrara, A. Kehagias and A. Riotto, arXiv:1405.2353;
K. Kamada and J. 'i. Yokoyama, arXiv:1405.6732;
K. Bamba, S.'i. Nojiri and S.D. Odintsov, arXiv:1406.2417.

[11] T. Li, Z. Li and D.V. Nanopoulos, arXiv:1405.0197;
J. Ellis, M. Garcia, D. Nanopoulos and K. Olive, *J. Cosmol. Astropart. Phys.* **05**, 037 (2014) [arXiv:1403.7518];
J. Ellis, M. Garcia, D. Nanopoulos and K. Olive, *J. Cosmol. Astropart. Phys.* **08**, 044 (2014) [arXiv:1405.0271].

[12] R. Kallosh, A. Linde and D. Roest, *J. High Energy Phys.* **11**, 198 (2013) [arXiv:1311.0472];
R. Kallosh, A. Linde and D. Roest, *J. High Energy Phys.* **08**, 052 (2014) [arXiv:1405.3646].

[13] B. Audren, D.G. Figueroa and T. Tram, arXiv:1405.1390.

[14] E. Cremmer, S. Ferrara, C. Kounnas and D.V. Nanopoulos, *Phys. Lett. B* **133**, 61 (1983);
J.R. Ellis, A.B. Lahanas, D.V. Nanopoulos and K. Tamvakis, *Phys. Lett. B* **134**, 429 (1984).

[15] C. Pallis, *J. Cosmol. Astropart. Phys.* **04**, 024 (2014) [arXiv:1312.3623].

[16] A. Kehagias, A.M. Dizgah and A. Riotto, *Phys. Rev. D* **89**, 043527 (2014) [arXiv:1312.1155].

[17] M.B. Einhorn and D.R.T. Jones, *J. High Energy Phys.* **03**, 026 (2010) [arXiv:0912.2718];
H.M. Lee, *J. Cosmol. Astropart. Phys.* **08**, 003 (2010) [arXiv:1005.2735];
S. Ferrara *et al.*, *Phys. Rev. D* **83**, 025008 (2011) [arXiv:1008.2942];
C. Pallis and N. Toumbas, *J. Cosmol. Astropart. Phys.* **02**, 019 (2011) [arXiv:1101.0325].

[18] S.V. Ketov and T. Terada, arXiv:1408.6524.

[19] S. Aoki and Y. Yamada, arXiv:1409.4183.

[20] I. Antoniadis, E. Dudas, S. Ferrara and A. Sagnotti, *Phys. Lett. B* **733**, 32 (2014) [arXiv:1403.3269];
S. Ferrara, R. Kallosh and A. Linde, arXiv:1408.4096;
R. Kallosh and A. Linde, arXiv:1408.5950.

[21] K. Enqvist and M. Karčiauskas, *J. Cosmol. Astropart. Phys.* **02**, 034 (2014) [arXiv:1312.5944].

[22] D.H. Lyth and A. Riotto, *Phys. Rept.* **314**, 1 (1999) [hep-ph/9807278];
A. Mazumdar and J. Rocher, *Phys. Rept.* **497**, 85 (2011) [arXiv:1001.0993].

[23] C. Pallis, *Phys. Lett. B* **692**, 287 (2010) [arXiv:1002.4765].

[24] D.H. Lyth, *Phys. Rev. Lett.* **78**, 1861 (1997) [hep-ph/9606387]; D.H. Lyth, arXiv:1403.7323.

[25] A. Kehagias and A. Riotto, *Phys. Rev. D* **89**, 101301 (2014) [arXiv:1403.4811].

[26] K.M. Smith, *et al. Phys. Rev. Lett.* **113**, 031301 (2014) [arXiv:1404.0373].